

Design and analysis of thermoplastic welded stiffened panels in post-buckling

van Dooren, K.S.; Bisagni, C.

Publication date

2021

Document Version

Final published version

Published in

Proceedings of the American Society for Composites, Thirty-Sixth Technical Conference

Citation (APA)

van Dooren, K. S., & Bisagni, C. (2021). Design and analysis of thermoplastic welded stiffened panels in post-buckling. In *Proceedings of the American Society for Composites, Thirty-Sixth Technical Conference* (pp. 406-417)

Important note

To cite this publication, please use the final published version (if applicable). Please check the document version above.

Copyright

Other than for strictly personal use, it is not permitted to download, forward or distribute the text or part of it, without the consent of the author(s) and/or copyright holder(s), unless the work is under an open content license such as Creative Commons.

Takedown policy

Please contact us and provide details if you believe this document breaches copyrights. We will remove access to the work immediately and investigate your claim.

Design and Analysis of Thermoplastic Welded Stiffened Panels in Post-Buckling

KEVIN S. VAN DOOREN and CHIARA BISAGNI

ABSTRACT

The Clean Sky 2 “SmarT mUlti-fuNctioNal and INtegrated TP fuselaGe” STUNNING project focusses on the next generation composite fuselage with emphasis on manufacturing techniques such as thermoplastic welding.

Welded multi-stringer panels are investigated in this paper, with emphasis on the buckling and skin-stringer separation behavior. The multi-stringer panels are designed to approximate the structural behavior of the lower half of the MultiFunctional Fuselage Demonstrator of the STUNNING project. In particular, a section of the fuselage is analyzed using Abaqus with a dynamic implicit analysis, and the results of this analysis are used for the design of the multi-stringer panels, taking manufacturing considerations also into account. The panels have three omega stringers and a length of 500 mm. The three stringer configuration allows to study the middle stringer in pristine and damaged configuration with minimal influence of the free edges and boundary conditions. It is seen that the multi-stringer test panels show very similar buckling and skin-stringer separation behavior compared to the fuselage section. The first panels have been manufactured by project partners NLR and GKN Aerospace Fokker and will be tested at the Faculty of Aerospace Engineering at Delft University of Technology.

Kevin S. van Dooren, Delft University of Technology, Faculty of Aerospace Engineering, 2629HS Delft, Netherlands.

Chiara Bisagni, Delft University of Technology, Faculty of Aerospace Engineering, 2629HS Delft, Netherlands.

INTRODUCTION

In the aeronautical field, composite structures usually consist of stiffened thin-walled designs which can present buckling under compression and shear loads. Allowing these structures to operate within the post-buckling field could lead to weight savings. However, this would require a higher understanding of the post-buckling behavior of composite structures and more specifically the failure mechanisms that can occur in the post-buckling field. The failure of composite structures is considered difficult to predict due to the complexity and catastrophic nature, leading to conservative designs and heavier structures.

In the post-buckling field it is seen that a common failure mode is skin-separation, caused by the high out-of-plane deformation of the skin. The research on skin-stringer separation is executed on several structural levels, with research conducted on multi-stringer panels [1-3], but also on single-stringer specimens for quasi-static loads [4-6] and fatigue loads [7-9]. Most of the research reported in literature is conducted on thermoset composites, which tends to fail more brittle compared to thermoplastic composites. Up to now thermoplastic composites are mainly researched in terms of manufacturing processes and design of structures [10,11], with limited research on predicting the buckling and post-buckling failure behavior.

The research presented in this paper is part of the Clean Sky 2 "SmarT mUlti-fuNctioNal and Integrated TP fuselaGe" STUNNING project. This project focusses on the development of thermoplastic composites for primary aeronautical structures, with emphasis on the development of a thermoplastic MultiFunctional Fuselage Demonstrator (MFFD) [12]. The fuselage makes use of thermoplastic welding in several critical joints.

A combined numerical and experimental methodology is in development to evaluate the strength of the welded joint between skin and stringer. In this paper test panels are designed by analysis, where the goal is to approximate the structural behavior of the lower half of the MFFD in the post-buckling field. To study the behavior of the welded joints in post-buckling on component level, a section of the MFFD is analyzed and the resulting structural behavior is used as a reference for the design process of the multi-stringer panels. The keel section of the fuselage is chosen as the area of interest, as it has a low skin thickness and is more susceptible to impact damage, for example due to tool drops. The test panel is then designed in an iterative manner to show similar structural and failure behavior with manufacturing and testing constraint also taken into account.

FUSELAGE SECTION GEOMETRY AND MATERIALS

The fuselage section is modelled to approximate the keel section of the MFFD up to the lower cargo-beams and with a length of three frame spacings. The keel-section of the MFFD is shown in Figure 1, and the fuselage section which approximates the keel section is shown in Figure 2. The frame spacing is 635 mm and the total length of the section is about 2 m. The outer radius of the skin is 1926 mm and the stringer pitch is 212 mm. The geometry of the omega stringer is shown in Figure 3. The total width of the section is 2664 mm. The skin and stringers are made of LMPAEK, for which information regarding material properties is limited. Therefore, material properties of a similar material, Toray CETEX TC1225 [13], are assumed with a ply thickness of 0.182 mm. The material properties of Toray CETEX TC1225 are shown in Table 1. The skin uses a 12 ply layup for the middle 9 bays and the two outer bays on each side have a 16 ply layup. The layup of the stringers consist of 9 plies. The different layups are shown in Table 2. The skin and stringers are joined together by conduction welding.

The fuselage section also includes other components such as the clips, brackets and frames among others. These components are simplified in the numerical model, as these will have less of an influence of the results and are not the main focus of this work.

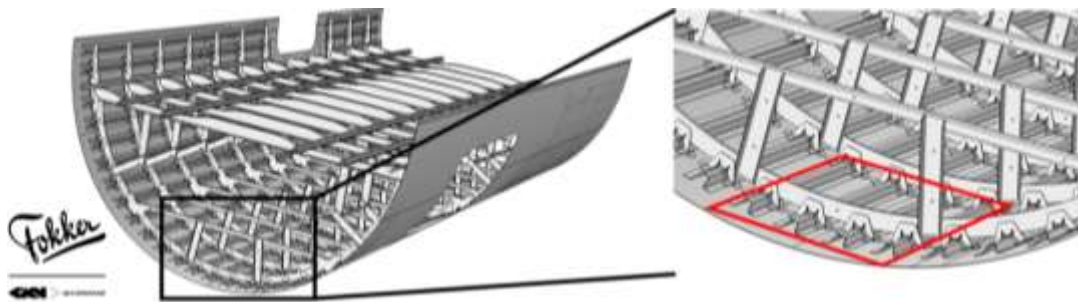


Figure 1. Lower half of the MultiFunctional Fuselage Demonstrator, highlighting the keel section.

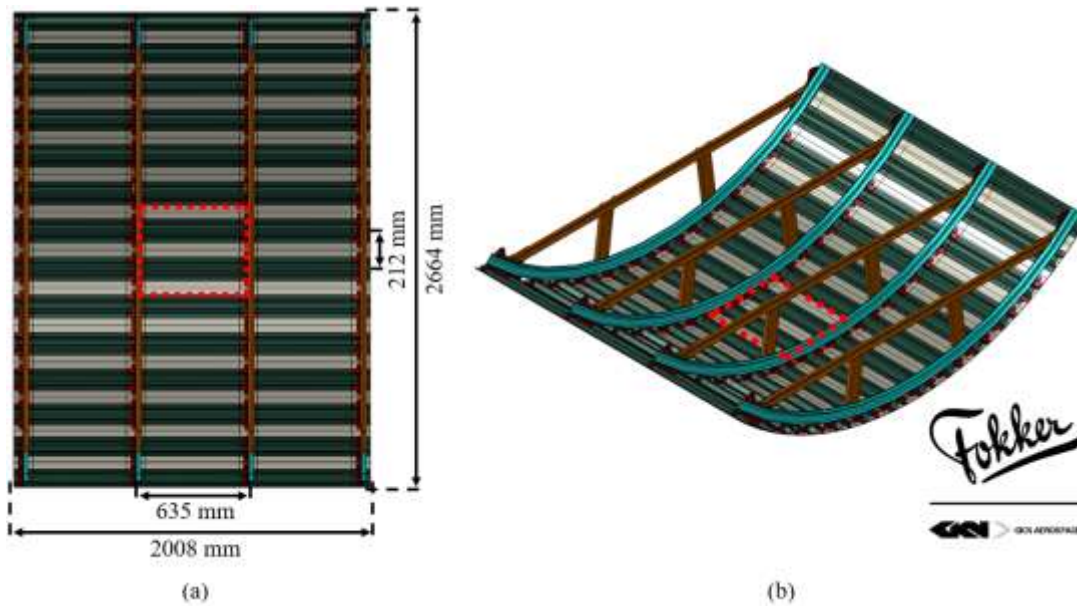


Figure 2. Fuselage section, with area of interest in red: (a): Top-view; (b): Iso-view.

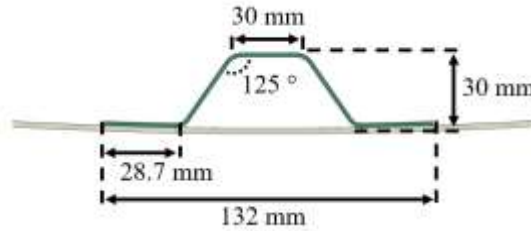


Figure 3. Omega stringer geometry.

TABLE I. LMPAEK TORAY CETEX TC1225 MATERIAL PROPERTIES [13].

E_{11} (MPa)	E_{22} (MPa)	ν_{12} (-)	G_{12} (MPa)
116800	9100	0.36	4100

TABLE 2. LAYUPS OF FUSELAGE SECTION.

NAME	LAYUP	THICKNESS (mm)
Skin 12	[-45,+45,0,90,-45,+45]s	2.12
Skin 16	[-45,+45,0,90,0,90,-45,+45]s	2.944
Stringer	[45,0,-45,0,90]s	1.656

MULT-STRINGER PANEL

The multi-stringer panels are designed to show similar structural behavior as the keel section of the MFFD, with the main focus on the buckling and failure behavior, and manufacturing constrains are also taken into account. The panels have three stringers, as shown in Figure 4, which allows to study the weld in both pristine and damaged condition with minimal influence of boundary conditions. A total of six flat panels will be manufactured and tested in three different configurations. The first

configuration is pristine, while the second and third configuration will have a damaged welded interface of the middle stringer with different damage locations.

The stringer geometry and pitch are the same as for the lower half of the MFFD, shown in Figure 3 and Figure 4 respectively. The panels have a width of 556 mm and a length of 500 mm. The length of the panels is according to the maximum welding length possible at the start of the design process. The panels are made of LMPAEK, for which the material properties are shown in Table 1. The layup of the stringer is the same as used in the lower half of the MFFD, but the skin layup is changed for a more conservative stress field in post-buckling. The layups are shown in Table 5.

The skin is manufactured by project partner NLR using automatic fiber placement followed by consolidation in an autoclave. Multiple skins are cut from a larger laminate to a size slightly larger than the final size. The stringers are joined to the skin by project partner GKN Fokker using conduction welding. After welding, the panels are cut to their final size. The last manufacturing steps consist of casting potting to both ends of the panels for load introduction and a final trim in a milling machine to minimize loading imperfections.

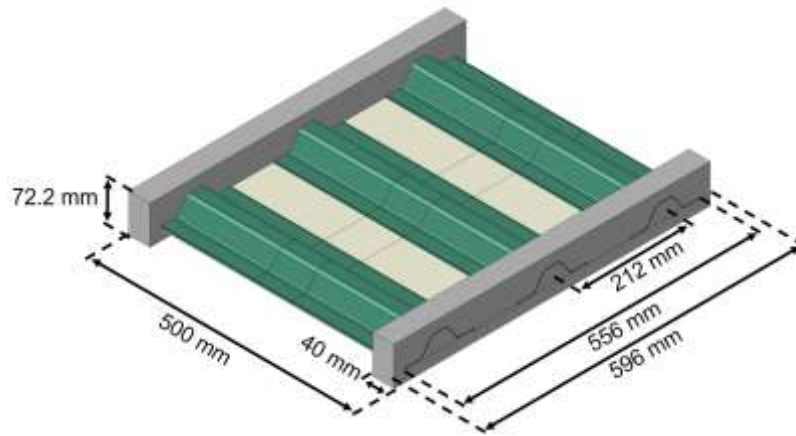


Figure 4. Multi-stringer panel.

TABLE 5. LAYUPS OF MULTI-STRINGER PANEL

NAME	LAYUP	THICKNESS (mm)
Skin	[-45,+45,0,90,-45,+45]s	2.12
Stringer	[45,0,-45,0,90]s	1.66

NUMERICAL METHODOLOGY

The numerical methodology uses the commercial software package Abaqus 2019 [14]. The fuselage section and multi-stringer panels are analyzed using dynamic implicit analysis. The load case for the panel consist of pure compression, which is applied by a displacement boundary condition. The fuselage section is loaded in bending by a linear displacement field boundary condition. The neutral bending axis runs parallel to the horizontal cargo-beams of the fuselage section and it goes through the center of the fuselage radius. Bending is applied such that the fuselage section is in compression, with the maximum compression being at the bottom of the section. The

free edges of the skin and free ends of the frames have the circumferential degree of freedom constraint, while the radial degree of freedom is not constraint.

The test panel uses a structured 2.5 mm mesh size for the laminated parts, while the potting material uses a variable mesh size between 2.5 and 10 mm to improve the computational efficiency. The mesh of the fuselage section is constructed such that the area of interest, which are the middle three bays in between the two middle frames as shown in Figure 2, are meshed with 2.5mm and the adjacent areas have a courser mesh of 5 mm where possible to improve computational efficiency. The cargo-beam and vertical strut have a mesh-size of 10 mm, and the brackets and clips have a mesh-size of 5 mm.

All laminated sections consist of the SC8R continuum shell element. The potting material of the test panel consists of the C3D8R solid element and the clips and brackets of the fuselage section use the C3D10 tetrahedral element.

Three different techniques are adopted to model joints between different geometries, namely rigid body ties, shared nodes and the Virtual Crack Closure Technique (VCCT). Rigid body ties are applied only in the fuselage section, to join parts which have mismatching meshes such as the cargo-beam, vertical strut, frame, clips and brackets.

The welded joint between the skin and stringer is modelled by either shared nodes or VCCT. VCCT is used for the two stringers in the main area of interest of the fuselage section as shown in Figure 2, and the adjacent areas use share nodes. The test panel utilizes VCCT in all three stringers in between the potting, while inside of the potting material all geometries are joined with shared nodes. VCCT is used in combination with the Benzeggagh-Kenane (BK) law model for mode-mixity. The mode I fracture toughness is based on preliminary material characterization within the STUNNING project, while the mode II, mode III and BK parameter are based on a similar material [15].

VCCT was chosen as it allows for a courser mesh to be used compared to other methods to model skin-stringer separation. The downside of VCCT is that it requires a pre-crack and is thus normally limited to damaged structures. However, the welded joint has a small unwelded area on each side of the joint which can be modelled as a pre-crack, as shown in Figure 5. This allows VCCT also to be applicable for pristine welded joints, and result in relatively computational efficient models for large structures.

First ply failure criteria are included in the analysis to check if material failure occurs before skin-stringer separation. The included criteria are Tsai-Hill, Tsai-Wu and Hashin. The strength properties are reported in Table 6 [13].

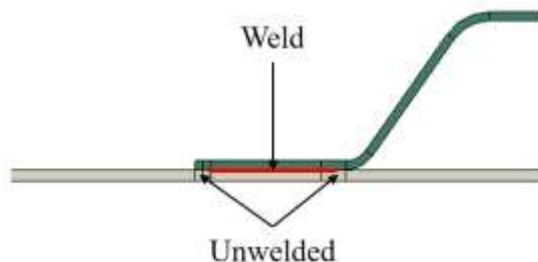


Figure 5. Weld between skin and stringer.

TABLE 6. LMPAEK TORAY CETEX TC1225 STRENGTH PROPERTIES [13].

F_{1T} (MPa)	F_{1C} (MPa)	F_{2T} (MPa)	F_{2C} (MPa)	F_{12} (MPa)
2442	1250	94	212	198

STRUCTURAL BEHAVIOR OF THE FUSELAGE SECTION

The global structural behavior of the fuselage section is investigated with emphasis on how the section buckles and on the evolution of the buckling shape till failure. Contour plots are shown at different levels of longitudinal bending, according to the maximum longitudinal displacement. Buckling starts in the middle bay between the two middle frames with a five half-wave buckling shape, see Figure 6(a), when the maximum longitudinal displacement is 5.35 mm. The buckling shape continuously evolves, with most bays showing a three half-wave buckling shape which evolves into a five half-wave buckling shape, see Figure 6(b). This evolution continues till almost all bays show a five half-wave buckling shape as shown in Figure 7(a). It is also seen that the side free edges are starting to show larger radial displacement, which might be caused by only constraining the circumferential degree of freedom. Failure due to skin-stringer separation in the area of interest occurs at a maximum displacement of 9.66 mm, for which the final buckling shape is shown in Figure 7(b).

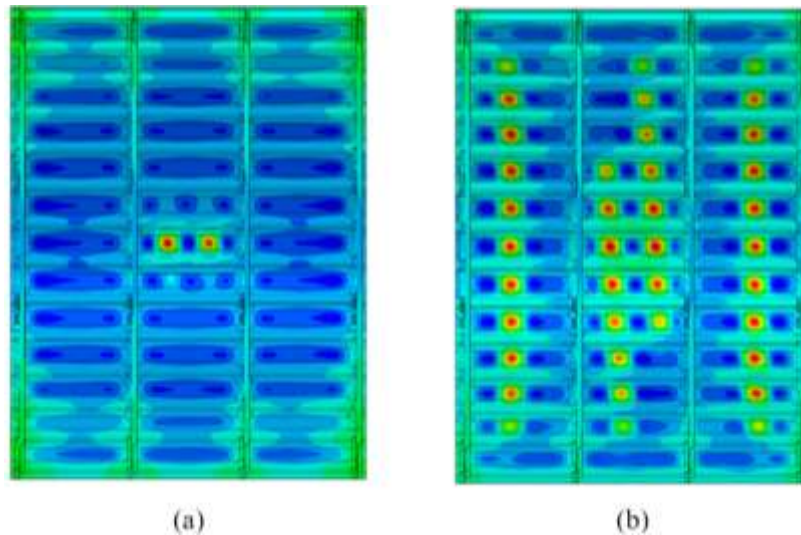


Figure 6. Fuselage section top-view contour plot showing radial displacement at different levels of bending: (a) Maximum displacement of 5.35 mm; (b) Maximum displacement of 7.01 mm.

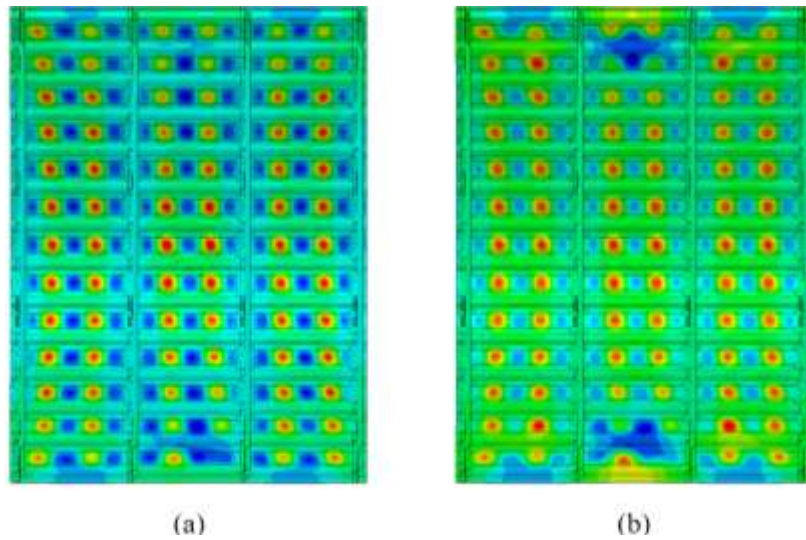


Figure 7. Fuselage section top-view contour plot showing radial displacement at different levels of bending: (a) Maximum displacement of 8.96 mm; (b) Maximum displacement of 9.66 mm.

To analyze the failure of the weld due to skin-stringer separation, the radial deformation and interface state in the area of interest, as shown in Figure 2, before failure and slightly into failure is studied in more detail. The area of interest is shown for the skin only with the stringers hidden, such that the buckling shape of both the bays and the skin underneath the stringer can be seen, with the outline of the stringer flanges shown in black. The radial displacement of this area just before failure is shown in Figure 8(a). The half-waves with the large radial displacement are in the bay area, while the smaller waves are underneath the stringers. It is seen that the half-waves underneath the stringer and in the bay have a similar half-wave length but the adjacent waves in circumferential direction do have opposite signs of radial displacement. Then, failure occurs due to skin-stringer separation first in the bottom stringer closely followed by the top stringer, which can be seen by the tunnels forming between outwards half-waves as shown in Figure 8(b). Both stringers show crack growth from underneath the stringer towards the bay, as shown by the skin-stringer interface in Figure 9, with an elliptical crack front. Once separation starts the growth is unstable and the stringer totally separates in one growth event.

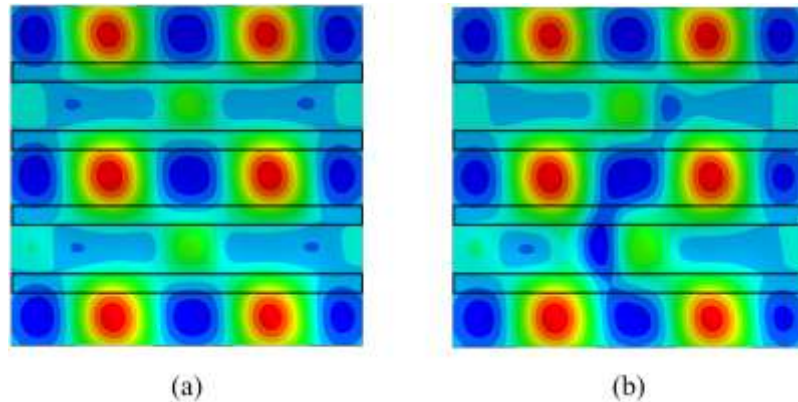


Figure 8. Area of interest top-view contour plot showing radial displacement at failure: (a) Just before failure; (b) During failure.

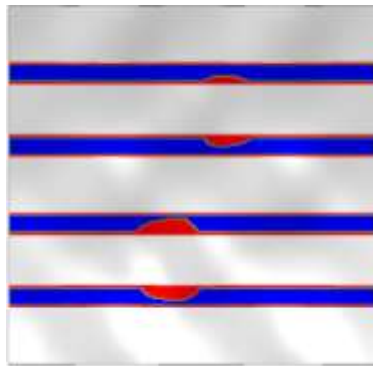


Figure 9. Stringer-interface in area of interest during failure, with intact interface in blue and separation in red.

PANEL STRUCTURAL BEHAVIOR

The structural behavior of the multi-stringer test panels is then analyzed in pristine condition and compared to the reference behavior of the fuselage section. First the load-displacement behavior is analyzed, followed by the buckling and failure behavior. The load-displacement graph of the multi-stringer panel is shown in Figure 10. The panel has a stiffness of 248.2 kN/mm until buckling at a load of 192 kN and displacement of 0.78 mm, which causes a reduction of stiffness. At a load of 341 kN and displacement of 1.48 mm another drop in stiffness is seen due to a small change in the buckling shape. The panel fails due to skin-stringer separation at a load of 389 kN and displacement of 1.76 mm.

The buckling shape consists of three half-waves, as shown in Figure 11(a), with two half-waves in outwards direction and one in inwards direction, while the fuselage section shows five half-waves for each frame spacing. The lower amount of half-waves is caused by the relatively short panel length, but the average half-wave length of both the test panel and the fuselage section is very similar. At a load of 341 kN the buckling shape changes underneath the stringer, with an increase in amount of half-waves as shown in Figure 11(b).

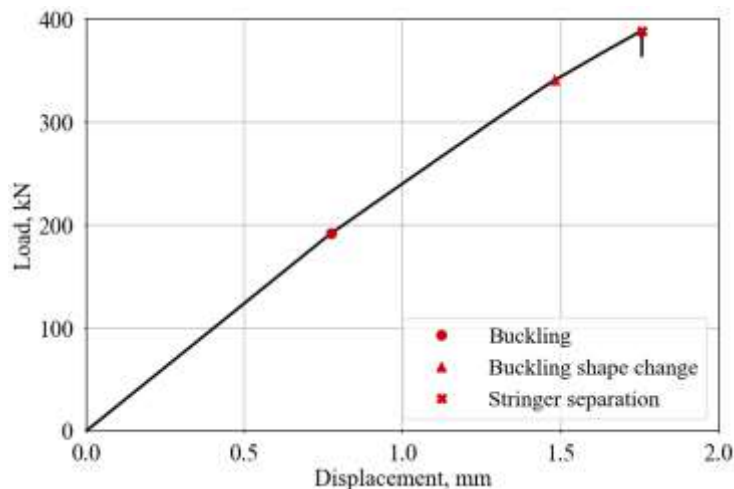


Figure 10. Load-displacement of the multi-stringer panel in pristine condition.

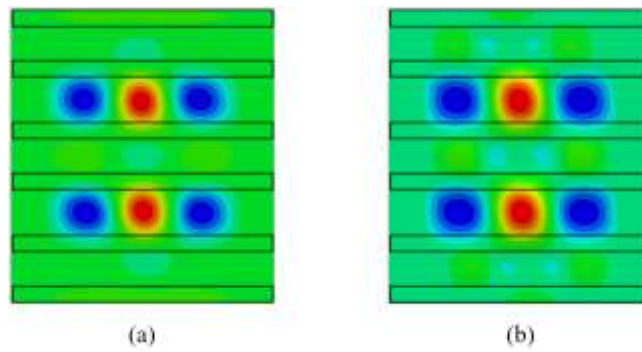


Figure 11. Buckling shapes of the panel at: (a) 0.78 mm; (b) 1.48 mm.

Two main aspects of the failure behavior as seen in the fuselage section and in the multi-stringer panel are compared: the out-of-plane deformation during failure and the shape and location of the crack front. Red dashed squares are used to highlight the areas with similar size and amount of half-waves in the bay. The out-of-plane deformation for the area of interest of the fuselage section and the test panel are shown in Figure 12(a) and 12(c) respectively. During failure both show a similar tunneling behavior underneath the stringer between inwards half-waves, as highlighted by the red squares. The fuselage section has one tunnel per red square, while the test panel has two tunnels forming. This is also seen on the interface in Figure 12(b) and 12(d) for the fuselage section and test panel respectively. The test panel exhibits the same crack growth behavior starting from underneath the stringer with an elliptical crack front as seen in the fuselage section. The number of failure locations is higher for the test panel, which seems to be caused by the difference in boundary conditions.

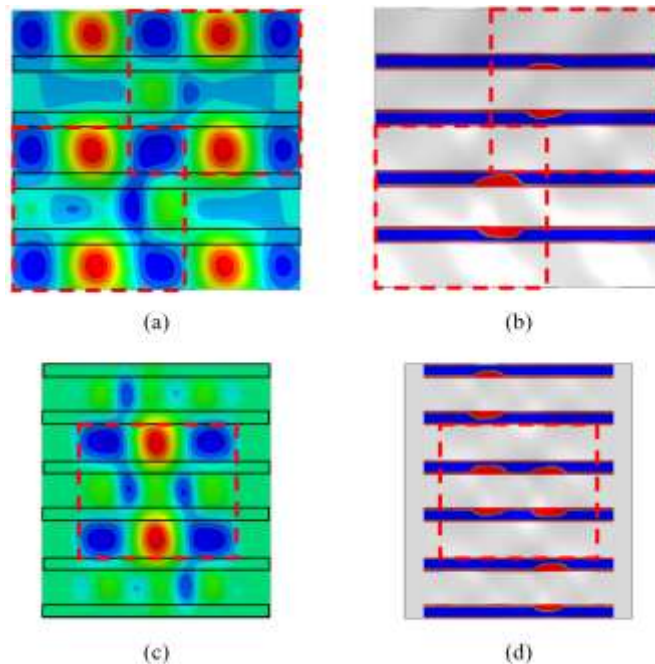


Figure 12. Comparison of failure behavior: (a) Buckling shape fuselage section; (b) Interface fuselage section; (c) Buckling shape panel; (d) Interface panel.

CONCLUDING REMARKS

In this paper a methodology is shown to investigate the strength of welded interface of thermoplastic stiffened structures, with the focus on the stiffened skin of the lower half of the MultiFunctional Fuselage Demonstrator of STUNNING. This study investigates the welded interface on sub-component level, for which multi-stringer test panels are designed. The keel section of the MFFD is considered to be the most critical section. A fuselage section representing the keel section is analyzed to determine the structural behavior, with emphasis on the buckling shape and skin-stringer separation behavior, which is used as a reference for the design of the multi-stringer panels.

The multi-stringer panels present a three stringer configuration, such that the welded interfaces of the middle stringer can be studied in both pristine and damaged condition, and have a length of 500 mm.

It is seen that the fuselage section shows a final buckling shape of five half-waves in each bay per frame spacing and fails due to skin-stringer separation. Crack growth starts from underneath the stringer causing tunneling between the outwards half-waves in the bay and underneath the stringer. The panel shows a buckling shape with a lower amount of half-waves, due to its shorter length, with similar half-wave length as seen in the fuselage section. The failure due to skin-stringer separation shows a high level of similarity compared to the fuselage section, but with a higher number of failure locations. The analysis of both the fuselage section and test panel show that similar structural behavior can be achieved on a lower structural level.

Manufacturing of the multi-stringer test panels has started by STUNNING project partners NLR and GKN Fokker and the panels will be tested at TU Delft. These tests allow to further study the welded interface with more detail, and validate the numerical methodology for both the buckling behavior and skin-stringer separation behavior.

ACKNOWLEDGEMENTS

This work is part of the STUNNING project and has received co-funding from the Clean Sky 2 Joint Undertaking (JU) under grant agreement No 945583. The JU receives support from the European Union's Horizon 2020 research and innovation programme and the Clean Sky 2 JU members other than the Union.



DISCLAIMER

The results, opinions, conclusions, etc. presented in this work are those of the author(s) only and do not necessarily represent the position of the JU; the JU is not responsible for any use made of the information contained herein.

REFERENCES

1. B. Falzon, K. Stevens, G. Davies. 2000. "Postbuckling behaviour of a blade stiffened composite panel loaded in uniaxial compression," *Composites: Part A*, 31: 459-468.
2. C. Meeks, E. Greenhalgh, B. Falzon. 2005. "Stiffener debonding mechanisms in post-buckled CFRP aerospace panels," *Composites: Part A*, 36: 934-946.
3. J. Bertolini, B. Castanié, J. Barrau, J. Navarro, C. Petiot. 2009. "Multi-level experimental and numerical analysis of composite stiffener debonding. Part 2: Element and panel level," *Composite Structures*, 90: 392-403.
4. C. Dávila, C. Bisagni. 2017. "Fatigue life and damage tolerance of postbuckled composite stiffened structures with initial delamination," *Composite Structures*, 161: 73-84.
5. R. Vescovini, C. Dávila, C. Bisagni. 2013. "Failure analysis of composite multistringers panels using simplified models," *Composites: Part B*, 45: 939-951.
6. N.R.Kolanu, G. Raju, M. Ramji. 2020. "A unified numerical approach for the simulation of intra and inter laminar damage evolution in stiffened CFRP panels under compression," *Composites Part B*, 190: 107931.
7. C. Dávila, C. Bisagni. 2017. "Fatigue life and damage tolerance of postbuckled composite stiffened structures with indentation damage," *Journal of Composite Materials*, 52(7): 931-943.
8. A. Raimondo, S. Doesburg, C. Bisagni. 2020. "Numerical study of quasi-static and fatigue delamination growth in a post-buckled composite stiffened panel," *Composites Part B*, 182: 107589.
9. C. Bisagni, C. Dávila. 2014. "Experimental investigation of the postbuckling response and collapse of a single-stringer specimen," *Composite Structures*, 19: 493-503.
10. V. Oliveri, G. Zucco, D. Peeters, G. Clancy, R. Telford, M. Rouhi, C. McHale, R. O'Higgins, T. Young, P. Weaver. 2019. "Design, manufacture and test of an in-situ consolidated thermoplastic variable-stiffness wingbox," *AIAA Journal*, 57(4): 1671-1683.
11. M. Flanagan, A. Doyle, K. Doyle, M. Ward, M. Bizeul, R. Canavan, B. Weaver, C. . Brádaigh, N. Harrison, J. Goggins. 2018. "Comparative manufacture and testing of induction welded and adhesively bonded carbon fibre peek stiffened panels," *Journal of Thermoplastic Composite Materials*, 32(12): 1622-1649.
12. S. Veldman, P. Kortbeek, P. Wölcken, R. Herrmann, J. Kos, I. Fernandez Villegas. 2020. "Development of a multifunctional fuselage demonstrator," *Aerospace Europe Conference*, Bordeaux.
13. Wichita State University, National Center for Advanced Materials Performance 2020 "Medium Toughness PAEK thermoplastics Toray (Formerly TenCate) Cetex® TC1225 (LM PAEK) T700GC 12K T1E Unidirectional Tape 145 gsm 34% RC Qualification Material Property Data Report", viewed 25-5-2020.
14. Dassault Systemes Simulia Corp 2019 "Abaqus 2019 documentation".
15. P. Camanho, C. Dávila, M. de Moura. 2003. "Numerical simulation of mixedmode progressive delamination in composite materials," *Journal of Composite Materials*, 37(16): 1415-1438.